Influence of nitrogen on the structure and nanomechanical properties of pulsed laser deposited tetrahedral amorphous carbon

2001 J. Phys.: Condens. Matter 13 2971

(http://iopscience.iop.org/0953-8984/13/13/311)

INSTITUTE OF PHYSICS PUBLISHING JOURNAL OF PHYSICS: CONDENSED MATTER

J. Phys.: Condens. Matter **13** (2001) 2971–2987 www.iop.org/Journals/cm PII: S0953-8984(01)20304-X

Influence of nitrogen on the structure and nanomechanical properties of pulsed laser deposited tetrahedral amorphous carbon

P Papakonstantinou[1] **and P Lemoine**

NIBEC, School of Electrical and Mechanical Engineering, University of Ulster at Jordanstown, Shore Road, Newtownabbey, Co Antrim BT37 OQB, Northern Ireland, UK

E-mail: p.papakonstantinou@ulst.ac.uk

Received 22 December 2000, in final form 19 February 2001

Abstract

The effect of nitrogen addition on the structure and nanomechanical properties of tetrahedral amorphous carbon, tα-C, has been studied. The tα-C films were grown on Al_2O_3–TiC substrates by reactive pulsed KrF excimer laser ablation of graphite targets at a laser fluence of 10 J cm^{-2}. Nitrogen contents up to 19 at.% were obtained by increasing the nitrogen partial pressure, P_{N_2}, to 75 mTorr. The sp^3 content in the tα-C film as determined by analysis of the XPS C 1s core level spectra had a value of about 76%. Incorporation of a small amount of nitrogen, 2 at.%, reduces the clustering of the sp^2 phase and improves the nanomechanical properties of the tα-C films, whilst for higher nitrogen concentrations the carbon bonding changes progressively from sp^3 to sp^2. Quantitative analysis of the Raman spectra indicated that incorporation of nitrogen greater than 2 at.% induced a progressive long-range order in the amorphous carbon and an increase in the size of sp^2 graphitic clusters. Additionally, Raman spectroscopy established the presence of C≡N bonds at high P_{N_2}. To elucidate the influence of the substrate on the measurement of the nanomechanical properties of thin film a continuous measure of hardness and modulus as a function of depth was performed. Both the hardness and Young's modulus were significantly reduced from 56 and 573 GPa for $CN_{0.02}$ to 2 and 44 GPa for $CN_{0.19}$ at a contact depth of 25 nm. The deterioration of the nanomechanical properties with N incorporation is consistent with the spectroscopic results, which indicate a structural transformation from an amorphous structure consisting predominately of sp^3 C bonds to an sp^2 graphitic-like phase.

(Some figures in this article are in colour only in the electronic version; see `www.iop.org`)

[1] Corresponding author: Dr Pagona Papakonstantinou.

1. Introduction

In the last decade amorphous carbon films have been intensively studied. This interest stems from the possibility of fabricating layers at low temperatures, with properties comparable to those of diamond [1, 2]. Diamond-like carbon, DLC, exhibits extreme hardness, IR transparency, chemical inertness and low friction, all of which have important technological applications. For example DLC has uses as hard coating for magnetic disk drives, antireflection coating for IR windows and cold cathodes for field emission displays. All these properties depend strongly on the short-range order of the structure such as bonding state of carbon atoms, the proportion of different bonding states and composition. In general amorphous carbon can have any mixture of sp^3 (tetrahedrally coordinated), sp^2 (trigonally coordinated) and sp^1 bonding configurations.

Amorphous carbon formed from highly ionized energetic species produced by techniques such as filtered cathodic arc [3], mass selective ion beam deposition [4] or pulsed laser deposition, PLD, [5, 6] can have sp^3 bonded fractions larger than 70%. This material is often referred to as tetrahedral bonded amorphous carbon, tα-C. It is widely believed that the high fourfold co-ordinated carbon content of tα-C films is the result of the sub-implantation of energetic incident carbon species beneath the growing film surface [7, 8]. This leads to localized regions of very high pressure extending several ångströms in depth.

High film hardness usually has been attributed to the presence of a high percentage of sp^3 (diamond) bonds whereas a high concentration of sp^2 (graphitic) bonds is regarded as leading to the formation of soft films [3, 9]. However, a new scenario appeared with the discovery of fullerines, carbon nanotubes and the fabrication of carbon films composed of sp^2 carbon with curved basal planes resembling fullerine structures [10] that can exhibit high hardness (up to 60 GP) and elastic recovery (up to 85%).

Many investigations have been dedicated to the introduction of additional elements such as fluorine, nitrogen, boron, silicon and various metals in the carboneous structure to modify the properties of conventional DLC coatings, in particular friction, wear, optical and electrical characteristics. The synthesis of carbon nitride has been the focus of intense experimental and theoretical effort since the prediction of hypothetical β-C_3N_4 [11] crystalline solids with mechanical properties superior to those of diamond. From a chemical point of view, the C_3N_4 phase should be very difficult to synthesize due to the well known trend of carbon and nitrogen to form multiply bonded compounds. Indeed, common to the majority of the techniques used is the production of an amorphous material, containing less than 57% nitrogen, required for the stoichiometric C_3N_4 and the difficulty in maintaining the sp^3 bonding as the nitrogen incorporation increases. Even though the synthesis of crystalline C_3N_4 has not been achieved, through all this research, amorphous sub-stoichiometric carbon nitride has emerged as a new material with both fundamental and practical interest.

Among the different phases known to date for the CN_x thin film system is the so called fullerine-like structure, synthesized at growth temperatures exceeding 200 °C [12]. This structure exhibits an unusual combination of hardness and elasticity, which has been attributed to curved and crosslinked graphitic basal planes, giving rise to a strong yet flexible three dimensional covalently bonded network.

The chemical structure of amorphous carbon nitride is still very poorly known. This is mainly due to the rich variety of possible local environments and the lack of long range order. The type of bonds present in the amorphous CN_x films is most commonly investigated using x-ray photoelectron spectroscopy. However a detailed and unambiguous description of the chemical structure is deficient as evidenced from the great spread of the obtained core level

binding energies in the literature [13, 14]. Also its relation to the nanomechanical properties still lacks a definitive interpretation.

Depth sensing indentation at low loads, or 'nanoindentation', has become an important method to obtain quantitative measurements of hardness (H) and Young modulus (E) on films microns to submicrons thick [15]. However, indentations with contact depths of less than 10% of the film thickness are needed to obtain intrinsic film properties and avoid the influence of the substrate [16]. Due to equipment limitations such as machine resolution, signal to noise ratio, inaccuracies in tip area calibration and incomplete subtraction of the Hertzian behaviour it is very difficult to obtain meaningful analytical results for indentation depths less than 20 nm [17]. Bearing in mind the above, it is obvious that it is not possible to obtain substrate independent results for films less than 200 nm thick (since 10% of 200 nm is 20 nm). Therefore, in order to analyse films less than 200 nm thick, it is essential to monitor the mechanical properties as a function of depth, in order to obtain an insight into the influence of the substrate.

The addition of nitrogen to tα-C pulsed laser deposited films, without the use of an additional energetic source, has been shown to have the following effects [18]. It causes a structural transformation of the sp^3 C bonded matrix into a relaxed polymeric configuration containing C=N bonds. Small additions of nitrogen (N/(C+N)$\sim$0.05) narrow the optical band gap (from 0.56 eV to 0.44 eV) and increase the electrical conductivity (from 5.8×10^{-4} to $1.9 \times 10^{-2}\ \Omega^{-1}\ \mathrm{cm}^{-1}$), whereas large additions lead to a wide band gap (>1.5 eV) and extremely low conductivity ($<1 \times 10^{-13}\ \Omega^{-1}\ \mathrm{cm}^{-1}$). Moreover, the nanomechanical hardness was found to decrease from $\sim$41 GPa for the pure tα-C to $\sim$1 GPa for the heavily nitrogenated films. On the other hand, an enhancement in the N–sp^3 C bonded sites was reported [19], when the N/C ratio increased from 0.3 to 0.4. However, in this case the rise in nitrogen concentration was achieved by increasing laser fluence and not by increasing the nitrogen background pressure.

This paper reports efforts to relate the chemical structure of carbon nitride thin films, deposited on Al_2O_3–TiC substrates, to their nanomechanical properties. A comparative analysis of the Raman [20] and XPS results has been performed in order to study the film composition and determine the type of bond formed in films produced by pulsed laser ablation in a controlled nitrogen atmosphere. We use a dynamic approach, termed continuous stiffness measurement [15], CSM, to continuously monitor the E and H values as a function of the indentation depths.

2. Experiment

Films were deposited using a KrF excimer laser ($\lambda = 248$ nm, repetition rate 10 Hz). The focused laser beam was incident at an angle of 45° to the target normal. The laser fluence was set at $10 \pm 0.5\ \mathrm{J\ cm}^{-2}$. At lower fluences (for e.g. less than $3 \pm 0.5\ \mathrm{J\ cm}^{-2}$) serious adherence problems were encountered when the films were exposed to atmosphere and therefore a high laser fluence of $10 \pm 0.5\ \mathrm{J\ cm}^{-2}$ was adopted for the experiments. The chamber was evacuated down to 4×10^{-3} mTorr prior to each deposition. Nitrogen gas (purity 99.999%) was admitted into the chamber during deposition. A mass flow controller in conjunction with a Baratron gauge was used to control the background nitrogen pressure inside the chamber. Films were fabricated with nitrogen partial pressures, P_{N_2}, of 0, 2, 4, 38 and 75 mTorr. The ablated material was collected on 10 mm $\times$ 10 mm segments of Al_2O_3–TiC substrate, placed at a distance of 40 mm from the target. Al_2O_3–TiC is a composite of titanium carbide (TiC) and alumina (α-Al_2O_3) in a 30:70 ratio and is the material used as head slider in magnetic recording heads. The substrates were cleaned ultrasonically with acetone, alcohol and methanol prior to loading and dried in flowing nitrogen. All the depositions were performed at room temperature.

Two series of CN_x coatings on Al_2O_3–TiC were produced under identical conditions but to different thicknesses of approximately 20 ± 7 nm and 150 ± 30 nm by controlling the number of laser pulses. The thickness of each sample was determined by an Alpha Step depth profiler and atomic force microscope. The thickness varied markedly along the sample. This is a common problem encountered in PLD, when stationary beam and substrate are used.

The XPS analysis was carried out in a XSAM 800 (KRATOS) spectrometer using a non-monochromated Mg Kα (1253.6 eV) x-ray source and a hemispherical electron energy analyser. The deconvolution of the C 1s and N 1s envelopes was performed using Gaussian line-shapes after Shirley background subtraction. Atomic percentages of each constituent were determined from the calculated areas under the corresponding Gaussian profiles corrected by instrumental sensitivity factors. Classically, sputter etching is used for cleaning before analysis. In our case all the spectra were recorded without a preceding sputter cleaning step.

Raman spectroscopy was used to provide information about the bonding nature of the threefold coordinated carbon atoms. Raman analysis was performed using a DILOR XY800 confocal micro-Raman spectrometer using 514.5 nm lines from an Ar ion laser. The spectra were taken over a range 600–3000 cm^{-1} with a resolution of 4 cm^{-1}.

All depth sensing indentation experiments were performed on a Nanoindenter XP (Nano Instruments) using the CSM option. The Berkovich tip area function was determined by indenting a standard fused silica sample of Young modulus equal to 726 GPa. The tip shape calibration procedure was repeated at the start and end of each experimental series run, to monitor any changes of the tip shape due to possible wear during testing. The nanoindenter continuously measures the load and displacement of a three sided pyramidal diamond indenter as it pushed into the sample. In the CSM mode [15] the indenter is loaded as in the standard mode but a small ac modulation is superimposed on the applied load. This enables the instrument to acquire continuously stiffness data from the load–displacement curves throughout the indentation process. The stiffness data permit the derivation of both hardness and modulus as a function of depth according to the Oliver and Pharr model. For each sample a series of 9 indents was performed, spaced 20 μm apart, and the results were averaged. The ac nano-indentations were performed under identical testing conditions, at maximum depths of 50 nm using a constant strain rate loading segment of 0.05 s^{-1}.

3. Results and discussion

3.1. Raman spectroscopy

Nitrogen partial pressures, P_{N_2}, of 0, 2, 4, 38 and 75 mTorr resulted in CN_x films with nitrogen content of 0, 2, 8, 17 and 19 at.% as measured by the x-ray photoelectron spectra. Nitrogen incorporation into the film is nearly linear with P_{N_2} at low P_{N_2} followed by a slower uptake of N at higher pressures. The slower uptake of N at higher pressures can be explained by the different plasma characteristics [21]. The majority of N is incorporated in the film by implantation of energetic CN species, formed directly in reactions involving energetic carbon species with the N_2 molecules. However, at high nitrogen pressures, numerous collisions of the incoming energetic carbon species with the N_2 molecules cause a confinement of the reaction region to distances much closer to the target surface, thereby reducing the formation of CN species. In addition the increased collisions slow down the energetic species and as a result the kinetic energy of plasma species is no longer sufficient to enhance the formation of the CN bonds. An efficient way to increase nitrogen incorporation is to use an extra plasma source to ionize the nitrogen gas.

Due to its sensitivity to changes in translational symmetry, Raman spectroscopy has proven a powerful tool for the study of disorder and crystalline formation in carbon-based materials. The Raman spectrum of diamond consists of a narrow band peaking at 1332 cm^{-1} while that of single crystal graphite consists of a narrow band peaking at about 1580 cm^{-1}. Polycrystalline graphite shows two relatively narrow Raman bands, a G band at approximately 1580–1600 cm^{-1} associated with the optically allowed zone vibrations (E_{2g} mode) of the aromatic ring in graphite and a D peak around 1350 cm^{-1} associated with disordered–allowed optical zone modes (A_{1g}) of microcrystalline graphitic sheets. The D peak is not present in perfect single crystal graphite and only becomes active in the presence of disorder. The Raman spectra of nanocrystalline and amorphous carbon are dominated by D and G peaks of varying intensity, position and width.

Figure 1 displays the Raman spectra, in the range 600–2000 cm^{-1}, of CN_x films approximately 150 nm thick, produced with various N contents. For 0 at.% N the sample exhibited a relatively symmetric broad peak near 1560 cm^{-1}. The broad band shape of the tα-C film suggests that its structure is amorphous. The strict selection rules for electronic transition set by the long-range translational symmetry of the crystal lattice are relaxed in the amorphous state and therefore more modes can contribute to Raman scattering resulting in the broadened Raman spectrum. It has been postulated that a visible Raman spectrum with a relatively symmetrical G band corresponds to high quality carbon film i.e. high sp^3:sp^2 ratio.

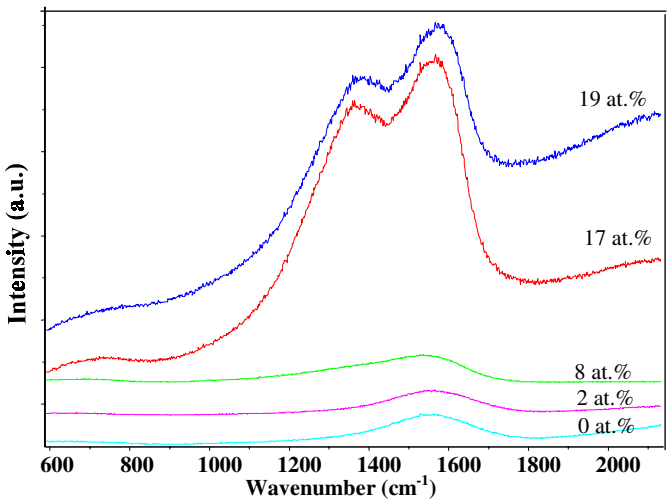

Figure 1. Micro-Raman spectra of 150 nm thick CN_x films with various nitrogen concentrations.

When a nitrogen amount of 8 at.% was incorporated into the film the asymmetry of the G band increased. At increased nitrogen levels of 17 and 19 at.% two distinct bands were resolved at 1575 cm^{-1} (G band) and 1375 cm^{-1} (D band). The G band (G for graphite) corresponds to graphite-like layers of sp^2 microdomains in the film, while the D band (D for disorder) is attributed to the bond angle disorder in the graphite-like microdomains, induced by the linking with sp^3 carbon atoms; the finite crystalline size of sp^2 nanodomains as well as substitutional N atoms and other impurities [22].

The Raman spectra of our films were quantitatively analysed using a computer code in order to reproduce the data as a sum of two Gaussians. Summarized in table 1 are the parametric

Table 1. Fitted Raman parameters of DLC and CN_x films ∼150 nm thick.

			G band (cm^{-1})		D band (cm^{-1})	
N (at.%)	P_{N_2} (mTorr)	I_D/I_G	Centre	FWHM	Centre	FWHM
0	0	0.25	1561	178	1408	247
2	2	0.21	1564	184	1400	273
8	4	0.78	1552	165	1377	308
17	38	1.14	1575	121	1374	257
19	75	1.03	1579	121	1375	235

values used in fitting the Raman spectra including the peak centre position for the D and G bands, as well as their respective bandwidth.

An initial increase of nitrogen content from 0 to 2 at.% shifted the G band from 1561 to 1564 cm^{-1} while its bandwidth increased from 178 to 184 cm^{-1}. Further, incorporation of N up to 8 at.% decreased G to 1552 cm^{-1}, after which it increased again. Its bandwidth reduced from 184 to 121 cm^{-1}. On the other hand as the nitrogen content increased from 0 to 19 at.%, the D band appeared to have shifted to lower wave numbers (1408–1375 cm^{-1}) while the corresponding bandwidth first increased and then dropped, exhibiting a maximum at 8 at.% N. When these data are compared with the corresponding G and D peak positions of graphite (1580 cm^{-1}, 1345 cm^{-1} respectively) material, it appears that with increasing N, both bands have shifted to wave numbers approaching those of graphite. Such a shift indicates that incorporation of nitrogen causes progressive graphitization in the tα-C films. This can be partly explained due to the increased collisional cooling of the ablation plume by the heavier nitrogen molecules leading to low impact energies on the substrate surface.

The width of the G peak is related to the bond angle disorder at sp^2 sites in the system [23]. The gradual narrowing of the G peak with increased N, indicates the development of long-range order in the a-C. Tetrahedral amorphous carbon films grown in the absence or in presence of a very small background nitrogen pressure (∼2 mTorr) have a higher degree of bond angle distortion most likely caused by the high particle energies.

In the tα-C film, the G peak dominates the overall fit and the intensity of the D peak, I_D, is very small. With increasing P_{N_2} the I_D is increasing relative to I_G. The evolution of I_D/I_G ratio is presented in table 1. The I_D/I_G ratio appears to decrease slightly with the N_2 partial pressure, when the P_{N_2} is extremely low (2 mTorr). Then it rises with the increase of P_{N_2} and reaches a maximum at 38 mTorr, after which it decreases again. The I_D/I_G ratio allows a qualitative characterization of the induced disorder in the sp^2 domains and this ratio is related to clustering of the sp^2 phase. The increase in the I_D/I_G suggests a lower disorder in the film. The dramatic rise in the I_D/I_G intensity ratio in effect corresponds to an increase in the number and size of disordered sp^2 sites according to the relationship [24]

$$\frac{I_D}{I_G} = C(\lambda)L_\alpha^2 \tag{1}$$

where L_α is the in plane crystallite size and C(514 nm)≈0.0028 for our films. On the other hand the small initial decrease in I_D/I_G suggests a reduction of sp^2 clustering. However this relationship is only valid for clustering of sp^2 sites with dimensions up to 20 Å. Above this crystallite size the I_D/I_G ratio starts to decrease and the Tuinstra and Koening relationship [25] is effective in which the ratio peak intensity varies inversely with L_α:

$$\frac{I_D}{I_G} = \frac{C(\lambda)}{L_\alpha}. \tag{2}$$

For nitrogen levels higher than 17 at.% a decrease in the I_D/I_G ratio was observed. This decrease is further substantiated in figure 2, which displays the I_D/I_G ratio for the two series of samples with thicknesses of approximately 150 and 20 nm respectively. It is clear that both series follow the same trend. This downward trend in I_D/I_G ratio at increased nitrogen pressures indicates further increase of the sp^2 cluster size as would be predicted by an application of the relationship (2).

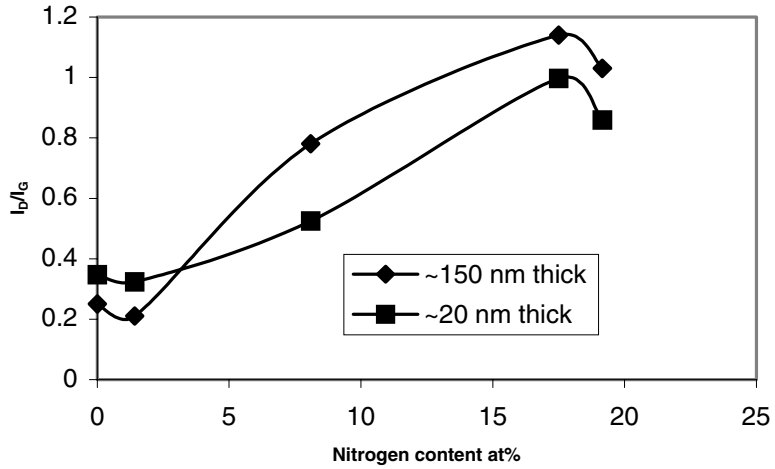

Figure 2. Dependence of I_D/I_G ratio on nitrogen concentration for 150 and 20 nm thick CN_x films.

It is obvious that in the above analysis no direct information on the sp^3 content of the films can be deduced from the visible Raman spectra. This is because visible Raman spectroscopy is ($\sim$55 times) more sensitive to sp^2 than sp^3 sites as visible photons are only able to excite π states. Recently direct observations of sp^3 bonding have come into practice by utilization of UV Raman spectroscopy [26], where shorter wavelengths were used to excite π and σ states, thus allowing a direct probe of both sp^2 and sp^3 bonding.

The films with high N concentration (17 and 19 at.%) exhibited a peak centred at about 2220 cm^{-1}, the intensity of which increased with N as illustrated in figure 3. This peak is attributed to C≡N bonds [19]. The development of C≡N sp^1 bonds at increased nitrogen pressures suggests that the nitrogen may play a role in terminating clusters in the film and weaken the film structure. The low frequency region of CN_x films is characterized by a broad peak at 690 cm^{-1}, which has been related to the disorder of the sp^2 carbon network [27]. The Raman active G and D bands become very prominent when large amounts of nitrogen (17 and 19 at.%) are present in the film. Strong enhancement of the Raman signal with increasing nitrogen pressure has been reported previously [28]. Kaufman *et al* [22] concluded that nitrogen substitution is responsible for the symmetry breaking of the E_{2g} mode and the intensity of the G and D bands.

3.2. X-ray photoelectron spectroscopy

In addition to carbon and nitrogen, oxygen (8 at.% O) was detected as a minor contamination (superficial) for samples containing nitrogen up to 8 at.%. In turn, a significant amount of oxygen (18 and 20 at.%) was found in the specimens containing a higher nitrogen concentration (17 and 19 at.%). The presence of oxygen is due to prolonged exposure of the samples

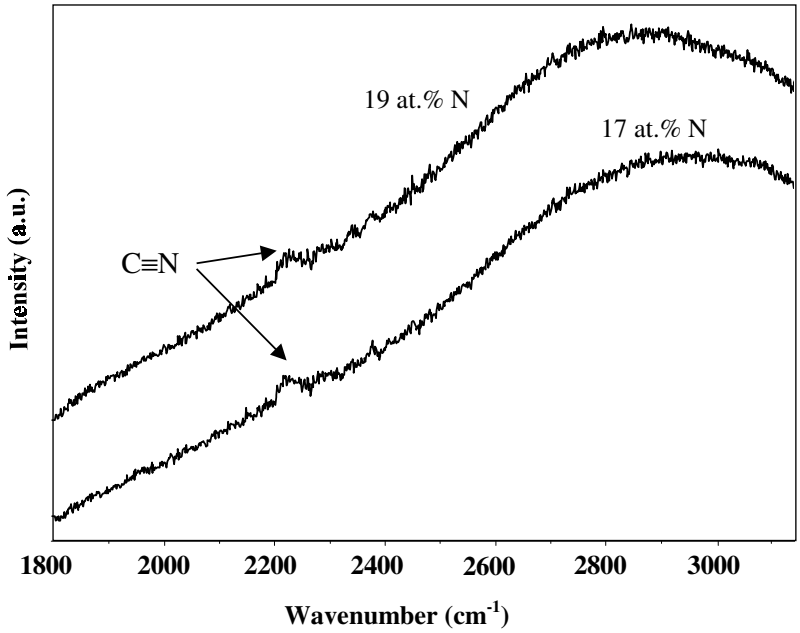

Figure 3. Micro-Raman spectra of $CN_{0.17}$ and $CN_{0.19}$ films in the high frequency range.

to the laboratory atmosphere. One explanation for the increased amount of oxygen in the high nitrogen content samples is to be found in the porosity and low density of the CN_x material. Tetrahedral CN_x films experience a reduction in mass density for increasing nitrogen concentrations. However, one should note that the presence of nitrogen in the carbon network and oxygen, resulting from the minor contamination, may also increase the electronegativity of the CN_x compound. As a result, the deposited films become more polar and tend to absorb H_2O molecules present in the laboratory atmosphere, therefore increasing the amount of oxygen present in the specimens.

The XPS analysis of the films revealed a very small chemical shift, with the C 1s peak positions of all the films deposited at different P_{N_2} remaining almost constant at 285.1 eV (figure 4(a)). The C 1s envelope of the DLC sample exhibited a narrow and regular shape, giving 1.6 eV as the width at half maximum. In turn, the nitrogen containing films showed broad and asymmetric C 1s envelopes at the higher binding energy side. The degree of asymmetry increased as a function of the nitrogen content, giving 1.6–3.3 eV as the width at half maximum, for the specimens containing 0–19 at.% nitrogen. This suggests that there are several bonding configurations related to carbon atoms in the films. No shift due to the charging effect was observed since the Al_2O_3–TiC is a conductive substrate. In addition, nitrogen incorporation is expected to increase the conductivity of the films. The N 1s envelopes, shown in figure 4(b) also exhibited a broad band centred at 399.5 eV binding energy.

Possible chemical bonding configurations were obtained by deconvoluting the individual C 1s and N 1s envelopes into Gaussian peaks. The best fits to C 1s and N 1s envelopes resulted in four and three Gaussian peaks respectively. The deconvoluted peaks of C 1s envelopes were located at binding energies of 284.5 ± 0.1, 285.2 ± 0.1, 286.5 ± 0.1 and 288.7 ± 0.1 eV, which are assigned to amorphous carbon C–C network, C=N, C–N or C≡N, and C–O [29, 30] bonds respectively. Likewise, N 1s envelopes were deconvoluted into three peaks at binding

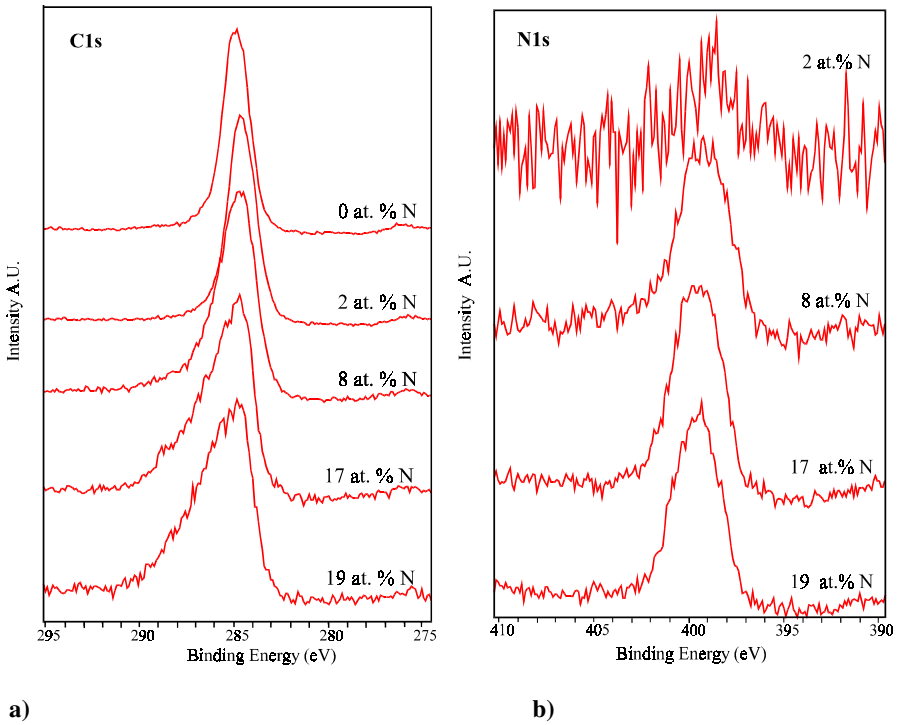

Figure 4. XPS (a) C 1s and (b) N 1s envelopes for a series of CN_x films with various nitrogen contents.

energies, BEs, of 398.5 $\pm$ 0.1, 400.1 $\pm$ 0.1 and 402 $\pm$ 0.1 eV, which are assigned to C–N or C≡N, C=N and N–O [29–31] bonds respectively.

A common observation in almost all the previous XPS studies of CN_x films is that the N 1s core level spectra are deconvoluted in two peaks located around binding energies of 398–398.6 and 399.8–401 eV and an insignificant third peak at about 402 eV related to N–O bonds. However, the assignment of the first two peaks is a matter of controversy. In the majority of studies, the low energy peak (398–398.6 eV) is attributed to C–N single bonds [29–31] or to C≡N triple bonds [32], while the high energy peak is attributed to C=N double bonds. Only a few authors have adopted the reverse assignment [13, 19]. The interpretation of our N 1s core level spectra is the most widely accepted in the literature.

The deconvolution of the C 1s envelopes in the literature, is even more controversial because they are symmetric and more than three peaks are necessary to distinguish the different bonding configurations. Also the position of the lines shifts if the substrate is nonconducting.

The decoconvoluted peaks of C 1s and N 1s envelopes for the specimen containing 8 at.% nitrogen are presented in figures 5(a) and 5(b) respectively. These values agree relatively well with referenced nitrogen containing organic polymers. For example, pyridine, C_5H_5N, which is a π bonded aromatic ring (C=N) with only one nitrogen atom has a C 1s BE of 285.5 eV [29, 31, 33, 34] and a N 1s BE of 399.8 eV [29, 33, 35]. In the tetrahedrally bonded nitrogen (C–N) containing compound, urotropine (or hexamethylene tetramine; $C_6H_{12}N_4$) the C 1s BE is 286.9 eV [29, 31, 33–36] and the N 1s BE is 399.4 eV [29, 31, 37]. Polyacronitrile, in which the only nitrogen atom forms one triple bond (C≡N) and one nonbonding lone pair of electrons, exhibits a C 1s BE of 286.4 eV [29, 33, 35, 38] and a N 1s BE of 399.6 eV [29, 33, 35, 38].

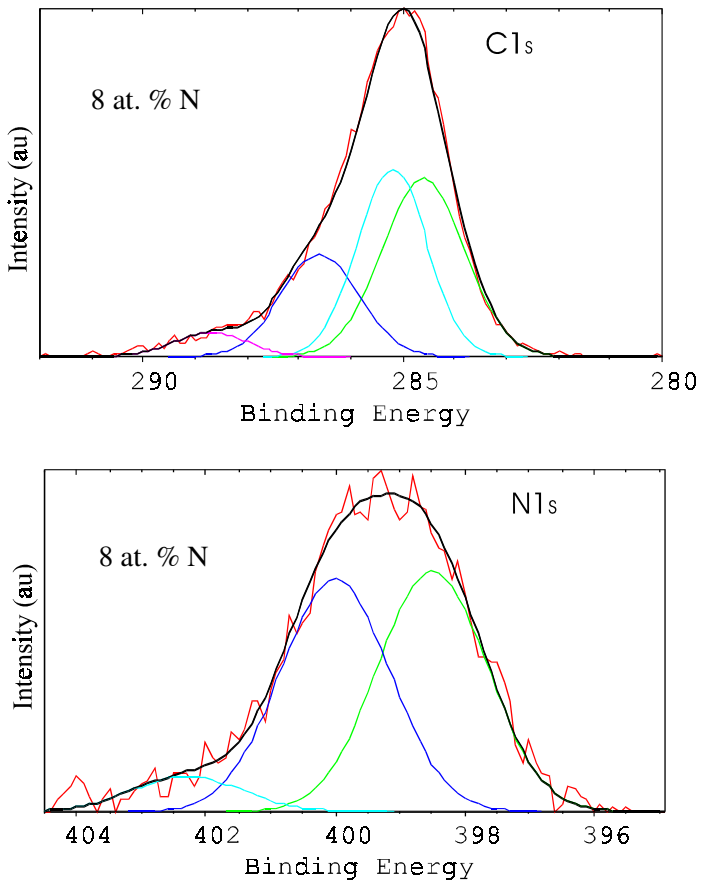

Figure 5. Deconvolution of C 1s and N 1s envelopes of a $CN_{0.08}$ film.

Table 2. Binding energy positions and the relative concentration (%) of the bonding types contributing to the XPS C 1s and N 1s envelopes.

	C 1s				N 1s		
	C–C	C=N	C–N	C–O	C–N	C=N	N–O
N (at.%)	284.5	285.2	286.5	288.7	398.5	400.1	402.0
8	43	25	29	37	47	46	7
17	16	30	42	12	21	67	12
19	13	31	43	13	20	70	10

Comparable assignments for both C 1s and N 1s envelopes have also been reported by Scarf *et al* [29] for sputtered deposited CN_x films ($x = 0.14$–0.18 at.%). The results of the curve fittings are presented in table 2, where peak positions and relative contributions of bonding types are summarized.

It is difficult to distinguish between C–N and C≡N bonding configurations since their binding energies are very close. However, it should be mentioned that although Raman spectroscopy identified the presence of C≡N bonds at high nitrogen concentrations (17 and 19 at.%) the signal was very small suggesting that C≡N bonds play only a minor role in the CN network.

The C 1s spectra of the tα-C and $CN_{0.02}$ films were deconvoluted into two main contributions at 284.4 eV and 285.2 eV (figure 6), which are respectively attributed to sp^2 and sp^3 coordinated carbon atoms [39]. A small peak at 287.4 eV was also present indicative of the binding state of C with O. From the deconvoluted spectra, the sp^3 content in both tα-C and $CN_{0.02}$ films was evaluated as ∼76%.

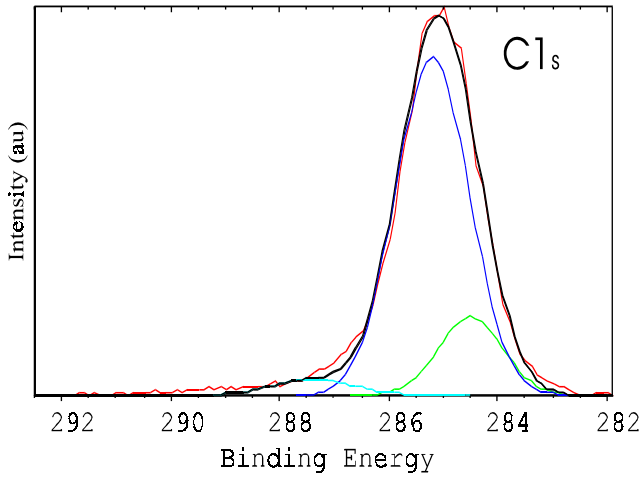

Figure 6. Deconvolution of C 1s envelope of a tα-C film.

The quantification of C 1s and N 1s envelopes resulting from the curve fitting highlights two major observations: (i) the nitrogen concentration in the deposited samples increases with P_{N_2} and is associated with a decrease of carbon to carbon bonding; (ii) the C=N bonding increases progressively at the expense of C–N. This result was confirmed by the FT–IR absorption analysis showing an increasing band at 1670 cm^{-1} as P_{N_2} rises. This is indicative [18, 40] of an increasing presence of N-sp^2 C vibrations in the specimens. The decrease in sp^3 C sites with increasing nitrogen pressure in the CN_x films is in agreement with other experimental works [41] based on energetic deposition conditions of CN_x films such as filtered cathodic arc. It is also in agreement with the subplantation model, bearing in mind that the kinetic energy of the ablated species decreases with P_{N_2} due to numerous collisions with the background N_2 molecules. Energetically, the sp^2 structure is the most favourable and the one attained unless additional excitation is provided.

The proposed bonding scheme permits us to explain the observed mechanical properties of the films, described in the next part, and is in agreement with the Raman and FTIR spectra.

3.3. Nanoidentation studies

Figure 7(a) presents the hardness as a function of the indentation contact depth for a series of CN_x films ∼150 nm thick. Data points represent the mean hardness values at specific indentation depths based on nine separate load/displacement tests. For the sake of comparison figure 7 also includes the results for an uncoated Al_2O_3–TiC substrate. For readability, error bars are shown only on the Al_2O_3–TiC substrate. Coating thickness can significantly affect the measured hardness. Since all films have approximately the same thickness and have been deposited on the same substrate we can rank the films in order of 'composite' hardness. The $CN_{0.02}$ and pure tα-C are the hardest followed by $CN_{0.08}$ and $CN_{0.17}$, which appear to be softer than the Al_2O_3–TiC substrate.

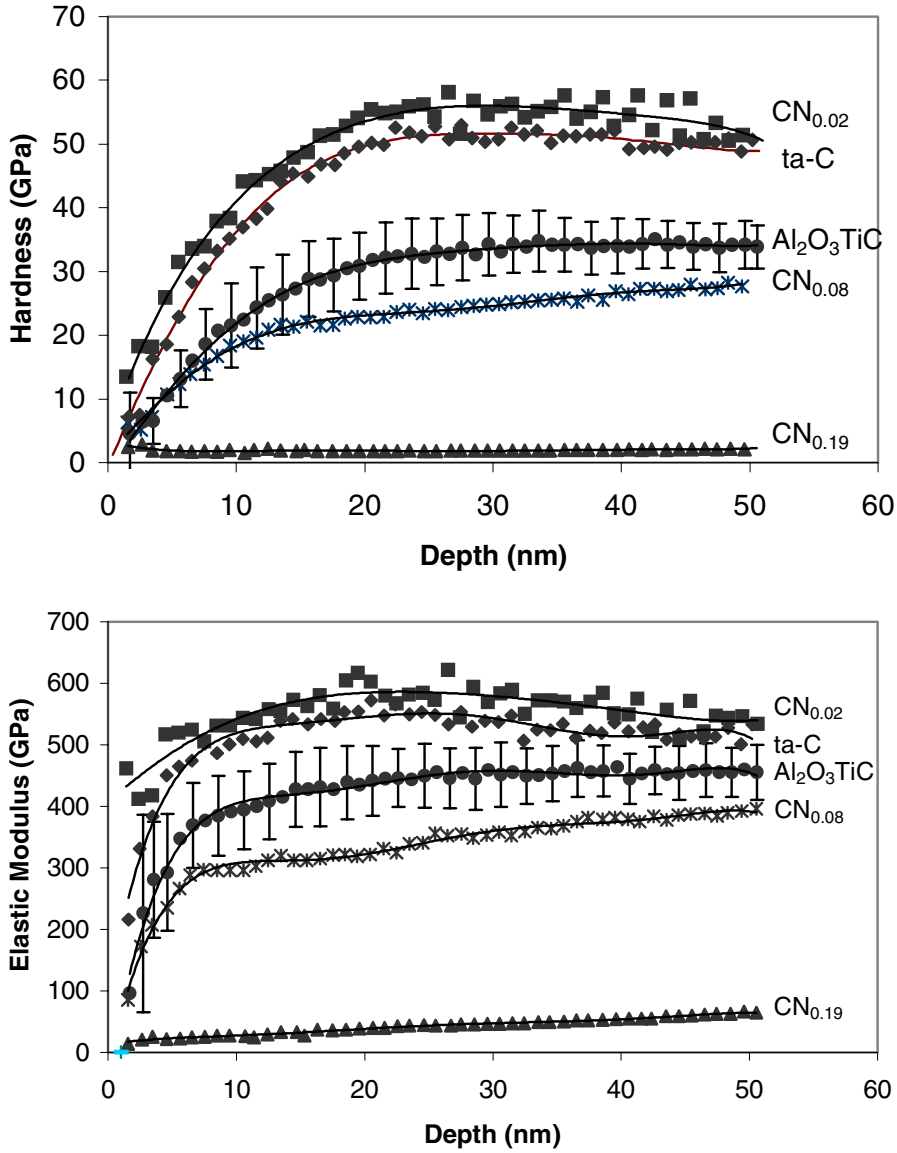

Figure 7. Hardness and elastic modulus against displacement of 150 nm thick CN_x films with various nitrogen concentrations.

Pure tα-C and $CN_{0.02}$ are particularly hard, exhibiting a hardness of approximately 52 and 56 ± 5 GPa at an indentation depth of 25 nm. This result shows that the incorporation of a small amount of nitrogen improves the mechanical properties probably by stabilizing the sp^3 bonding configuration. This finding is in agreement with the Raman spectra, which show a slight decrease in the I_D/I_G ratio (from 0.25 to 0.21) with increasing nitrogen composition to 2 at.%. Such hard films may cause tip wear. Therefore checking the condition of the tip was an important part of the procedure. One would expect that if the tip were being progressively blunted the displacement at a given load would decrease successively. To check that the tip

geometry was stable through the series of tests, we measured the hardness of a standard bulk silica sample before and after each experiment. No noticeable differences were observed, suggesting no appreciable tip wear, probably because the tip was not sharp.

In the hardness curves two stages can be clearly resolved. First the hardness increases as the indentation increases up to 20 nm. Second, for indentation depths higher than 20 nm hardness decreases/increases to values approaching those of the Al_2O_3–TiC substrate. The rising behaviour in the first stage can be explained taking into account that hardness is calculated assuming plastic deformation from the first contact between the sample and the indenter. It is expected that for small loads the deformation of the sample is purely elastic. Thus hardness is calculated from uncorrected depths without introducing the elastic recovery, which reaches high values in the elastic region. The limitations to characterize the geometry (contact area) of the indenter tip at extremely shallow depths should also be taken into account.

The observed decrease/increase in hardness with indentation depth in the second stage (displacement >20 nm) is due to a substrate influence. This behaviour is caused by the increasing plastic deformation of the Al_2O_3–TiC substrate as the indenter is pushed deeper into the sample. The calculated hardness data are also affected by the sink in effects and the deformation of the indenter in the hard film/soft substrate systems (such as tα-C and $CN_{0.02}$) and pile-up effects in soft film/hard substrate ($CN_{0.08}$ and $CN_{0.17}$).

The $E(d)$ curves shown in figure 7(b) display similar features. As the indentation depth increases the elastic modulus increases/decreases, approaching that of the Al_2O_3–TiC substrate (430 GPa). These results indicate that the CN_x films with N contents of 8 and 17 at.% are elastically less stiff than the substrate.

It was immediately noticed that the standard deviation of both H and E on the Al_2O_3–TiC substrate was much larger than that on silica substrate. The dual phase of Al_2O_3–TiC is responsible for the relatively large standard deviations in the mean values of H and E. An AFM image of a tα-C coated Al_2O_3–TiC substrate is given in figure 8. The topography of the film resembles that of the substrate. The higher features correspond to the hard TiC phase while the background corresponds to the soft Al_2O_3 phase. Obviously mechanical polishing preferentially removes the Al_2O_3 resulting in the rough surface. The TiC crystalline regions (30%) are 0.5–2 μm wide and much harder than the surrounding Al_2O_3 matrix. Thus the random placement of the indenter is bound to give different deformations for these two regions. The roughness of the substrate could also be a contributing factor in the measured standard deviation of H and E.

The hardness and elastic modulus values at a penetration depth of 25 nm are $(52, 553)$, $(56, 580)$, $(23, 350)$, $(1, 44)$ and $(30, 455)$ for the tα-C, $CN_{0.02}$, $CN_{0.08}$, $CN_{0.17}$ and Al_2O_3–TiC substrate respectively. Both the hardness and Young modulus appear to increase slightly with nitrogen partial pressure when P_{N_2} is extremely low. Then H and E continuously decrease with further increase of P_{N_2} as does the sp^3 content. Similar trends in the nanomechanical properties have been observed in CN films prepared by cathodic arc [41]. The high hardness of the tα-C is attributed to the presence of a high percentage ($\sim$76%) of sp^3 bonds. Highly sp^3 tα-C films can be viewed structurally as a rigid matrix consisting of sp^3 bonds in which short chains of sp^2 sites are embedded. Initial introduction of nitrogen (2 at.%) at very low P_{N_2} leads to a reduction in the size of sp^2 clusters. However at increased P_{N_2}, further addition of nitrogen leads to an increase in the size of sp^2 clusters and the rigidity of the carbon network is substantially reduced. The structural changes are related to the kinetic energy of the deposited plasma species. At low P_{N_2} high energies promote densification of the carbon network and increase the hardness. The dramatic decrease in the nanomechanical properties at high background nitrogen pressures is attributed to the thermalization of the laser ablated species, leading to the formation of structures with reduced three dimensional cross linking. In addition, formation

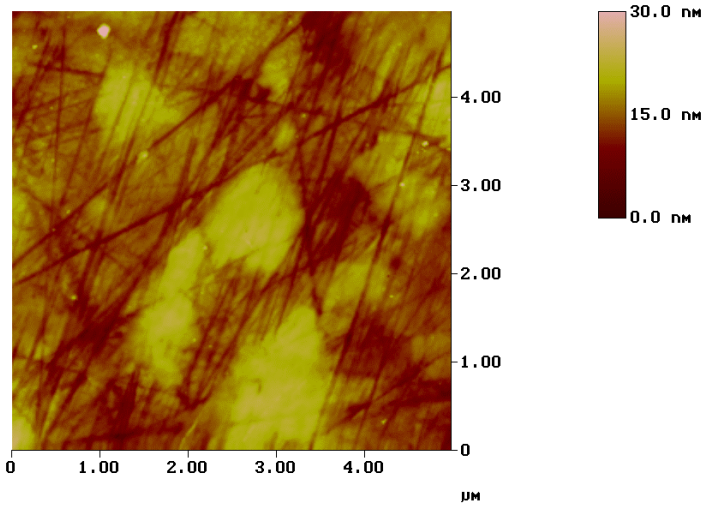

Figure 8. AFM image of a tα-C coated Al_2O_3–TiC substrate.

of terminating C≡N bonds interrupts the network connectivity, thus substantially reducing the nanohardness of the material. The results show that the incorporation of nitrogen at high levels reverts the sp^3 network to sp^2, exhibiting the soft characteristics of graphite since only the weak Van der Waals bonds would be acting between the basal planes [42].

The H/E ratio drops from 0.1 to 0.02 as the nitrogen content increases from 2 to 19%. The ratio H/E, which is used as a measure of the material's ability to resist plastic deformation in a contact event, indicates that the tα-C and $CN_{0.02}$ films are the most resistant. This dramatic decrease in hardness and Young modulus after heavy nitrogen incorporation on PLD carbon films has been reported previously; however no detailed nanomechanical characterization was performed.

The hardness and elastic modulus curves of tα-C films of different thickness 150, 100, 50 and 20 nm are plotted together in figure 9 in order to illustrate the effect of the thickness dependence on the mechanical properties of these films. The thinner films show a reduced hardness. For Al_2O_3–TiC covered with 50 nm tα-C no appreciable hardening effect could be detected. The increase in H value is only significant for films thicker than 50 nm.

The $H(d)$ and $E(d)$ curves for $CN_{0.08}$ and $CN_{0.17}$ films of thicknesses 150 and 20 nm are presented in figure 10. It can be seen that all the coatings decrease the hardness of the substrate, with the thicker films showing the larger softening effect. The $CN_{0.08}$ samples are harder than the $CN_{0.17}$ irrespective of thickness. The larger $H(d)$ slope of the thin 20 nm $CN_{0.17}$ sample merely reflects that the effect of the substrate is more pronounced while the smaller slope of the thick 150 nm $CN_{0.17}$ sample shows that the measured hardness is largely due to the film itself.

4. Conclusions

We have investigated the effect of nitrogen partial pressure on the chemical bonding structure and nanomechanical properties of laser pulse deposited, PLD CN_x films. In summary PLD CN_x films with nitrogen content up to 19 at.% were grown onto Al_2O_3–TiC substrates by increasing P_{N_2} up to 75 mTorr. The sp^3 content in pure tα-C and $CN_{0.02}$ films as determined

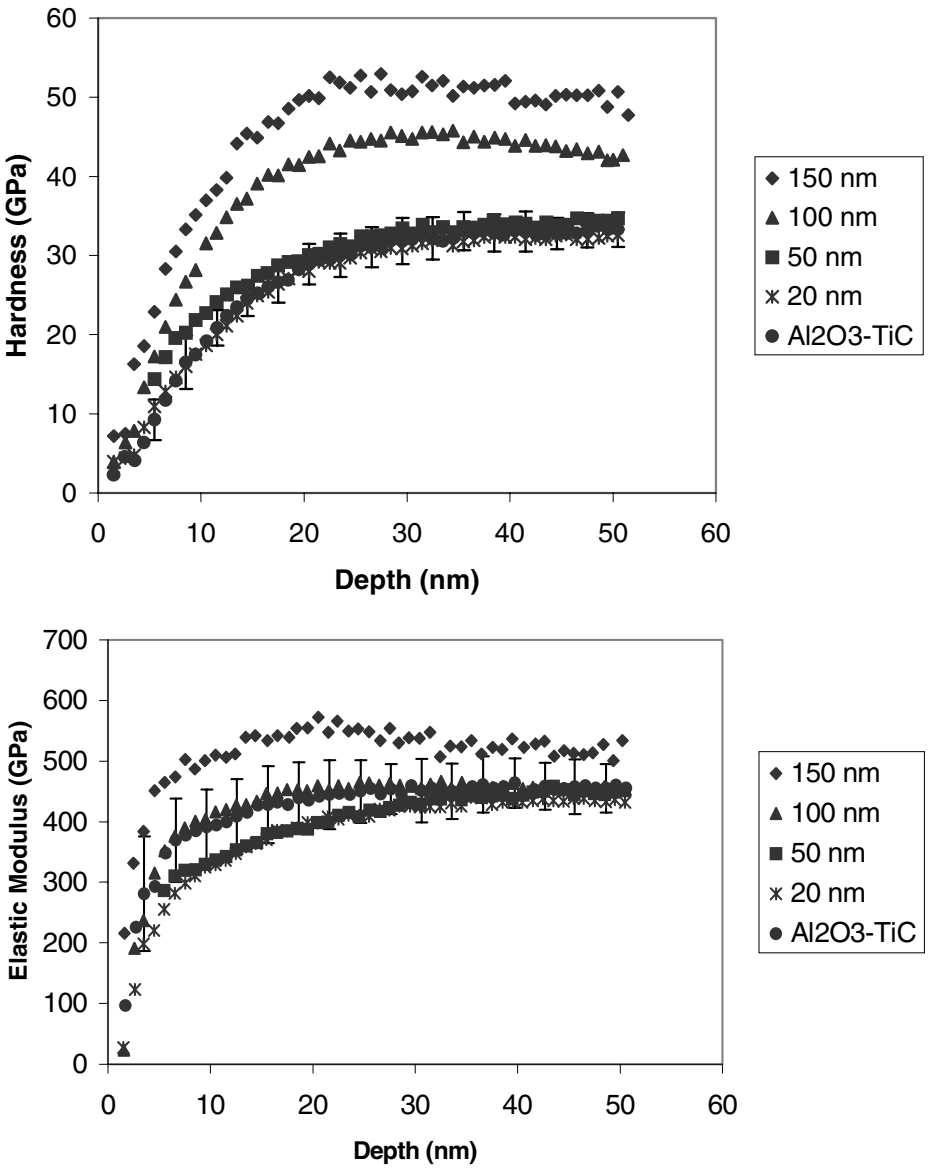

Figure 9. Hardness and elastic modulus against displacement of tα-C films with various thicknesses.

by analysis of the XPS C 1s core level spectra had a value of about 76%. Quantitative analysis of the Raman spectra indicated that slight incorporation of N (2 at.%) reduced the clustering of the sp^2 phase; however further increase in nitrogen induced a progressive long-range order in the amorphous carbon and an increase in the size of sp^2 graphitic clusters. In addition, Raman spectroscopy established the formation of C≡N bonds at high P_{N_2}. The XPS results confirmed a preferential formation of C=N bonds. Both hardness and Young modulus appeared to increase slightly when a small amount of nitrogen was introduced into the tα-C films. Further addition of nitrogen decreased H and E and reached very low values at the highest N content

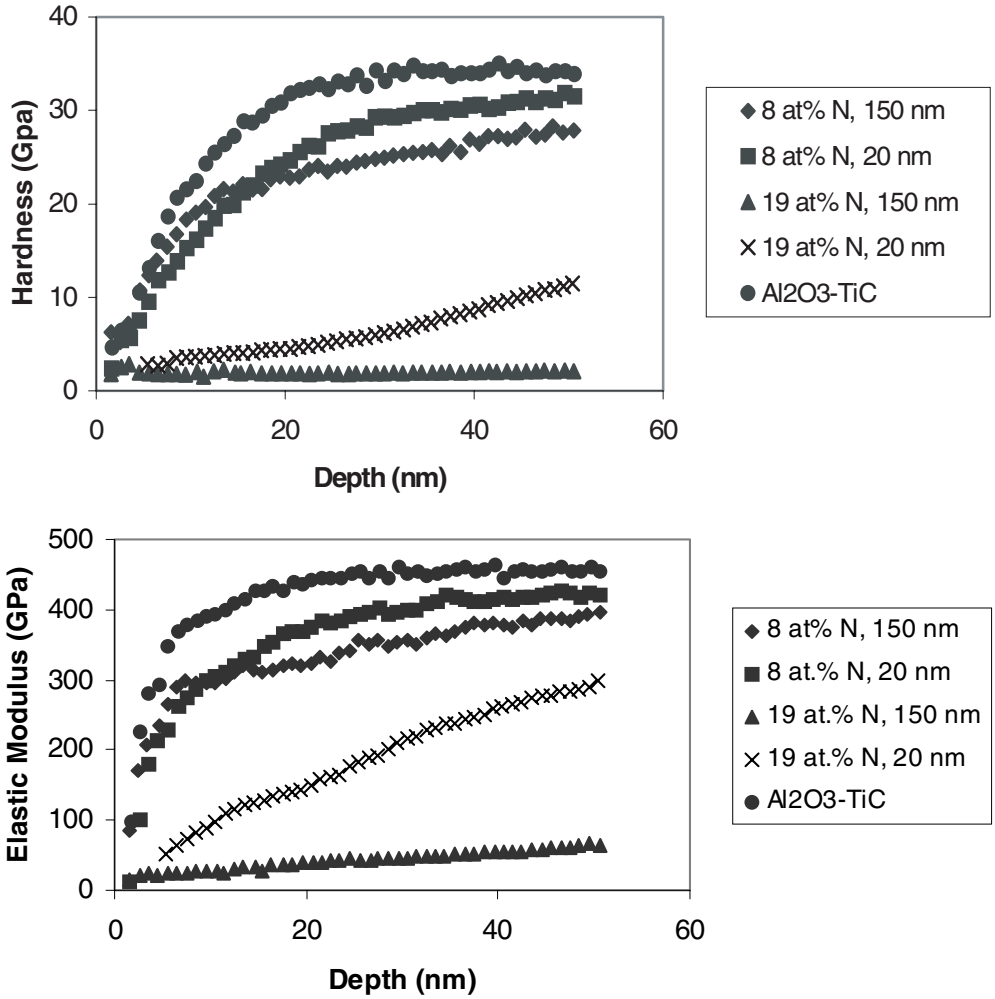

Figure 10. Hardness and elastic modulus against displacement of $CN_{0.17}$ and $CN_{0.19}$ films with thicknesses of 150 and 20 nm.

of 19 at.%. The deterioration of the nanomechanical properties is attributed to a transition from an amorphous structure consisting of predominately sp^3 C bonds to a graphitic phase consisting predominately of double bonded C and N atoms.

Acknowledgments

One of the authors (PP) would like to acknowledge the grant G503/20259/JE from the Royal Society. This work was supported by the European Union through the 'ultraviolet laser facility' at the Institute of Electronic Structure and Laser Applications in Crete, contact No ERBFMGECT 950021. The author would like to thank Dr A Zeze for carrying out the XPS measurements.

References

[1] Grill A 1999 *Diamond Relat. Mater.* **8** 428
[2] Robertson J 1991 *Prog. Solid State Chem.* **21** 199
[3] Fallon P J, Veerasamy V S, Davis C A, Robertson J, Amaratunga G A J and Milne W I 1993 *Phys. Rev.* B **48** 4777
[4] Hofsass H, Binder H, Klumpp T and Recknagel E 1994 *Diamond Relat. Mater.* **3** 137
[5] Voevodin A, Donley M S and Zabinski J S 1997 *Surf. Coat. Technol.* **52** 42
[6] Davanloo F, Jungerman E M, Jander D A, Lee T J and Collins C B 1990 *J. Appl. Phys.* **67** 2081
[7] Lifshitz Y, Kasi S R and Rabalais J 1989 *Phys. Rev. Lett.* **68** 620
[8] Robertson J 1994 *Diamond Relat. Mater.* **3** 361
[9] Xu S, Flynn D, Tay B K, Prawer S, Nuget K W, Silva S R P, Lifshitz Y and Milne W I 1997 *Phil. Mag.* B **76** 351
[10] Alexandrou I, Scheibe H J, Kiely C J, Papworth A P, Amaratunga G A J and Schultrich B 1999 *Phys. Rev.* B **60** 10 903
[11] Liu A Y and Cohen M 1989 *Science* **24** 841
[12] Sjostrom H, Stafstrom S, Boman M and Sundgren J E 1995 *Phys. Rev.* B **75** 1336
[13] Ronning C, Feldermann H, Merk R, Hofsass H, Reinke P and Thiele J U 1998 *Phys. Rev.* B **58** 2207
[14] D'Anna E, De Giorgi M L, Luches A, Martino M, Perrone A and Zocco A 1999 *Thin Solid Films* **347** 72
[15] Oliver W C and Pharr G M 1992 *J. Mater. Res.* **7** 1564
[16] Pharr G M and Oliver W C 1998 *Mater. Res. Soc. Symp. Proc.* vol 505 (Pittsburgh, PA: Materials Research Society) p 65
[17] Hay J C, Bolshakov A and Pharr G M 1999 *J. Mater. Res.* **14** 2296
[18] Zhao X A, Ong C W, Tsang Y C, Wong Y W, Chan P W and Choy C L 1995 *Appl. Phys. Lett.* **66** 2652
[19] Riedo E, Comin F, Chevrier J and Bonnot A M 2000 *J. Appl. Phys.* **88** 4365
[20] Tamor M A and Vassell W C 1994 *J. Appl. Phys.* **76** 3823
[21] Vivien C, Hermann J, Perrone A, Boulmer-Leborgne C and Luches A 1998 *J. Phys. D: Appl. Phys.* **31** 1263
[22] Kaufman H, Metin S and Sapaerstein D D 1989 *Phys. Rev.* B **39** 13 053
[23] Dilon R O, Woollam J A and Katkanant V 1984 *Phys. Rev.* B **29** 3842
[24] Ferrari A C and Robertson J 2000 *Phys. Rev.* B **61** 14 095
[25] Tuinstra F and Koening J L 1970 *J. Chem. Phys.* **53** 1126
[26] Gilkes K W R, Sanda H S, Batchelder D N, Robertson J and Milne W I 1997 *Appl. Phys. Lett.* **70** 1980
[27] Lacendra M M, Franceschini D F, Freire F L Jr, Achete C A and Mariotto G 1997 *J. Vac. Sci. Technol.* A **15** 1970
[28] Chowdhury A K M S, Cameron D C and Hashmi M S J 1998 *Thin Solid Films* **332** 62
[29] Scarf T W, Ott R D, Yang D and Barnard J A 1999 *J. Appl. Phys.* **85** 3142
[30] Sjostrom H, Hultman L, Sundgren J E, Hainsworth S V, Page T F and Theunissen S S A M 1996 *J. Vac. Sci. Technol.* A **14** 56
[31] Marton D, Boyd K Y, Al-Bayati A H, Todorov S S and Rabalais J W 1994 *Phys. Rev. Lett.* **73** 118
[32] Rossi F, Andre B, Vanveen A, Mijnarends P E, Schut H, Labohm F, Dunlop H, Delplancke M P and Hubbard K 1994 *J. Mater. Res.* **9** 2440
[33] Bhattacharya S, Cardinaud C and Turban G 1998 *J. Appl. Phys.* **83** 3917
[34] Barber M, Connor J A, Guest M F, Hiller I H, Schwarz M and Stacey M 1973 *J. Chem. Soc. Faraday Trans.* II **69** 551
[35] Mansour A and Ugolini D 1993 *Phys. Rev.* B **47** 10 201
[36] Gelius U, Heden P F, Hedman J, Lindberg B J, Manne R, Nording R and Siegbahn K 1970 *Phys. Scr.* **2** 70
[37] Lindberg B J and Hedman J 1975 *Chem. Scr.* **7** 155
[38] Beamson G and Briggs D 1992 *High Resolution XPS of Organic Polymers* (New York: Wiley)
[39] Tabbal M, Merel P, Chaker M, El Khakani M A, Herbert E G, Lucas B N and O'Hern M E 1999 *J. Appl. Phys.* **85** 3860
[40] Lu Y F, Ren Z M, Song W D, Chan D S H, Low T S, Gamani K, Chen G and Li K 1998 *J. Appl. Phys.* **84** 2909
[41] Davis C A, McKenzie D R, Yin Y, Kravtchinskaia E, Amaratunga G A J and Veerasamy V S 1994 *Phil. Mag.* B **69** 1133
[42] Hu J T, Yang P D and Lieber C M 1998 *Phys. Rev.* B **57** R3185